













Engineered magnetization and exchange stiffness in direct-write Co–Fe nanoelements

Cite as: Appl. Phys. Lett. **118**, 022408 (2021); <https://doi.org/10.1063/5.0036361>

Submitted: 04 November 2020 . Accepted: 21 December 2020 . Published Online: 15 January 2021

 S. A. Bunyaev,  B. Budinska, R. Sachser,  Q. Wang,  K. Levchenko,  S. Knauer,  A. V. Bondarenko,  M. Urbánek,  K. Y. Guslienko,  A. V. Chumak,  M. Huth,  G. N. Kakazei, and  O. V. Dobrovolskiy



View Online



Export Citation



CrossMark

ARTICLES YOU MAY BE INTERESTED IN

[Evidence of phonon pumping by magnonic spin currents](#)

Applied Physics Letters **118**, 022409 (2021); <https://doi.org/10.1063/5.0035690>

[Introduction to spin wave computing](#)

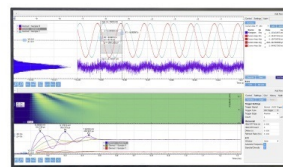
Journal of Applied Physics **128**, 161101 (2020); <https://doi.org/10.1063/5.0019328>

[Control of magnetic anisotropy in a Co thin film on a flexible substrate by applying biaxial tensile strain](#)

Applied Physics Letters **118**, 022406 (2021); <https://doi.org/10.1063/5.0035003>

Challenge us.

What are your needs for periodic signal detection?



Zurich Instruments



Engineered magnetization and exchange stiffness in direct-write Co-Fe nanoelements

Cite as: Appl. Phys. Lett. **118**, 022408 (2021); doi: 10.1063/5.0036361

Submitted: 4 November 2020 · Accepted: 21 December 2020 ·

Published Online: 15 January 2021



View Online



Export Citation



CrossMark

S. A. Bunyaev,¹ B. Budinska,² R. Sachser,³ Q. Wang,² K. Levchenko,² S. Knauer,² A. V. Bondarenko,¹ M. Urbánek,⁴ K. Y. Guslienko,^{5,6} A. V. Chumak,² M. Huth,³ G. N. Kakazei,¹ and O. V. Dobrovolskiy^{2,a)}

AFFILIATIONS

¹Institute of Physics for Advanced Materials, Nanotechnology and Photonics (IFIMUP)/Departamento de Física e Astronomia, Universidade do Porto, 4169-007 Porto, Portugal

²Faculty of Physics, University of Vienna, 1090 Vienna, Austria

³Physikalisches Institut, Goethe University, 60438 Frankfurt am Main, Germany

⁴CEITEC BUT, Brno University of Technology, 61200 Brno, Czech Republic

⁵Division de Física de Materiales, Depto. Polímeros y Materiales Avanzados: Física, Química y Tecnología, Universidad del País Vasco, UPV/EHU, 20018 San Sebastian, Spain

⁶IKERBASQUE, The Basque Foundation for Science, 48009 Bilbao, Spain

^{a)} Author to whom correspondence should be addressed: oleksandr.dobrovolskiy@univie.ac.at

ABSTRACT

Media with engineered magnetization are essential building blocks in magnonics, spintronics, and superconductivity. However, the established thin film and lithographic techniques insufficiently suit the realization of planar components with on-demand-tailored magnetization in the lateral dimension. Here, we demonstrate the engineering of the magnetic properties of CoFe-based nanodisks fabricated by the mask-less technique of focused electron beam-induced deposition (FEBID). The material composition in the nanodisks is tuned *in situ* via the e-beam waiting time in the FEBID process and their post-growth irradiation with Ga ions. The saturation magnetization M_s and exchange stiffness A of the disks are deduced from perpendicular spin-wave resonance measurements. The achieved M_s variation in the broad range from 720 emu/cm³ to 1430 emu/cm³ continuously bridges the gap between the M_s values of widely used magnonic materials such as Permalloy and CoFeB. The presented approach paves the way toward nanoscale 2D and 3D systems with controllable space-varied magnetic properties.

© 2021 Author(s). All article content, except where otherwise noted, is licensed under a Creative Commons Attribution (CC BY) license (<http://creativecommons.org/licenses/by/4.0/>). <https://doi.org/10.1063/5.0036361>

Magnonics—the study of spin waves and their use in information processing systems—has emerged as one of the most rapidly developing research fields of modern magnetism.^{1–10} Now, its key challenges are guiding and control of spin waves in 1D (e.g., magnonic crystals^{11–14}), 2D (e.g., magnonic circuits^{8,9}), and emerging 3D systems.^{7,15,16} For steering of spin waves, one should change an external parameter such as magnetic field^{5,17–19} and temperature^{20–22} or alter the conduit shape^{11,23,24} and magnetization.^{22,25–29} Among these approaches, magnetization variation has an advantage if being passive (no current or heat involved) and it can be strongly localized or gradient-tailored on purpose. Thus, *in situ* approaches for tuning magnetization in a broad range are strongly demanded. In this regard, ion irradiation-induced evolution of the magnetic parameters of thin films and nanostructures has been a matter of extensive research.^{29–35}

Focused electron beam-induced deposition (FEBID) can offer unique features, which go beyond the state-of-the-art fabrication technologies of magnonics.³⁶ First, the down to 10 nm lateral resolution (for selected materials, such as Co-Fe alloys³⁷ discussed in what follows) makes FEBID suitable for the fabrication of nanostructures with feature sizes comparable to modern complementary metal-oxide semiconducting (CMOS) technology. Second, the composition and magnetic properties of FEBID nanostructures can be tuned via post-growth irradiation of structures with ions^{24,38} and electrons.^{39,40} In addition, FEBID is capable of fabricating complex-shaped 3D nanoarchitectures,^{41,42} which make it the technique of choice for studies in superconductivity,^{43–45} magnetism,^{46–48} and magnonics.^{7,15,16}

In a previous study, we observed the decrease in the magnetization M_s and the exchange stiffness A with reduction of the diameter of

individual Co–Fe nanodisks.⁴⁹ The effect was attributed to the writing of smaller disks in a depleted-precursor regime, which results in a lower metal content. Here, we introduce a beam waiting time outside of written structures to demonstrate on-demand engineering of the magnetization and exchange stiffness in individual Co–Fe nanodisks with a thickness of 40 nm and a larger fixed radius $R = 500$ nm. In our studies, one series of nanodisks was fabricated using different e-beam waiting times in the FEBID process and another series of nanodisks was irradiated with different doses of Ga ions. The magnetization M_s and exchange stiffness A of the disks were deduced from spin-wave resonance (SWR) measurements, employing a recently developed spatially resolved approach.⁴⁹ We demonstrate that with an increase in the e-beam waiting time, M_s of the disks reaches 1430 emu/cm^3 , which is by a factor of two larger than M_s of the disks irradiated with Ga ions. Thus, the combination of these two approaches provides access to the fabrication of geometrically uniform magnonic conduits with a drastic variation of saturation magnetization.

The circular Co–Fe disks were fabricated by FEBID in a high-resolution dual-beam scanning electron microscope (SEM: FEI Nova NanoLab 600) employing $\text{HCo}_3\text{Fe}(\text{CO})_{12}$ as precursor gas.^{37,50} FEBID was done with 5 kV/1.6 nA, 20 nm pitch, and 1 μs dwell time, using a serpentine scanning strategy, see Fig. 1(a). All disks were written with 1632 beam passes, deduced from a thickness calibration by atomic force microscopy (AFM). Two series of samples used in our studies are described next.

The first series of samples is a set of four disks deposited onto a Si/SiO₂ (200 nm) substrate, written with different beam waiting times. After each pass of the electron beam over the disk surface, the beam was “parked” for the time τ varied from $\tau_0 = 0$ to $\tau_3 = 50$ ms outside of the disk. The essential steps of the writing process are illustrated in Fig. 1(a). All disks from the first series exhibit a flat morphology, Fig. 1(d). The thickness variation for the disks written with different τ_i did not exceed 0.5 nm.

The substrate was mounted onto a translational stage for their face-to-face positioning under the 2- μm -wide and 6- μm -long active part of an Au coplanar waveguide (CPW), Fig. 1(c). The CPW was prepared by e-beam lithography from a 55-nm-thick Au film dc-magnetron-sputtered onto a Si/SiO₂ (200 nm) substrate with a 5-nm-thick Cr buffer layer. The CPW was covered with a 5-nm-thick TiO₂ layer for electrical insulation from the disks. SWR measurements on both sample series were taken at the fixed frequency of 9.85 GHz with the magnetic field oriented perpendicularly to the disk plane, Fig. 1(c).

The second series of samples refers to four states of a disk written with $\tau_0 = 0$ on the CPW and irradiated with 30 keV Ga ions up to a cumulative dose D_3 of $15 \text{ pC}/\mu\text{m}^2$ in steps of $5 \text{ pC}/\mu\text{m}^2$, Fig. 1(b). SRIM simulations of the distribution of 30 keV Ga ions implanted in the Co–Fe disks indicate that it has a gentle-dome shape spreading through the entire disk thickness, with the largest number of stopped Ga ions in the depth range from 13 nm to 28 nm, see the inset in Fig. 1(b). In consequence of the ion irradiation, the disk thickness decreased to $36.8 \pm 0.5 \text{ nm}$ for $D_3 = 15 \text{ pC}/\mu\text{m}^2$, Fig. 1(d), which was accompanied by an increase in the surface roughness.

For the analytical description of the field values of resonance peaks, we considered azimuthally symmetric spin-wave modes in a thin cylindrical disk saturated in the out-of-plane direction by the biasing magnetic field H . In this case, the excited spin-wave eigenmodes can be described by Bessel functions of the zeroth order because of the axial

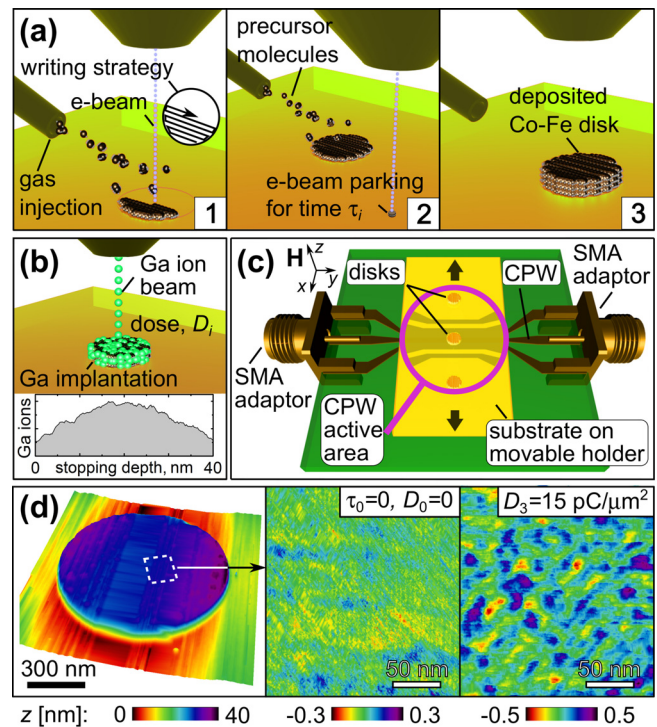


FIG. 1. (a) Illustration of the FEBID process for the first series of disks: after each pass over the sample surface (1), the beam is parked outside of the disk for the given time τ_i (2). The writing process is continued until the desired disk thickness is achieved (3). (b) In the second series of measurements, a Co–Fe disk is irradiated by 30 keV Ga ions with different doses D_i . Inset: simulated distribution of stopped Ga ions across the disk thickness. (c) Experimental geometry (not to scale). A substrate with a series of Co–Fe nanodisks is placed face-to-face to a gold coplanar waveguide for spin-wave excitation in the out-of-plane bias magnetic field H . (d) Atomic force microscopy image of the reference disk ($\tau_0 = 0$, $D_0 = 0$) and its surface morphology in comparison with the ion-irradiated disk with $D_3 = 15 \text{ pC}/\mu\text{m}^2$.

symmetry of the samples. The details of the analytical theory can be found elsewhere.⁵¹ This approach allows for the deduction of M_s and A with high precision.

Figure 2 presents the experimentally measured SWR spectra as a function of the out-of-plane magnetic field H for the disks irradiated with different doses of Ga ions and the disks deposited with different electron beam waiting times. In all cases, the most intense resonance peak is observed at the largest field that corresponds to the lowest spin-wave mode number $n = 1$. On the low-field side, the main resonance is accompanied by a series of peaks with a monotonously decreasing amplitude. Such a spin-wave spectrum is typical for confined circular nanodots.⁵¹ We observe that the two used approaches lead to shifts of the SWR fields in opposite directions with respect to the reference state ($D_0 = 0$, $\tau_0 = 0$). At the same time, the shape and the intermodal distance pattern evolve consistently, which is indicative of compositional uniformity and magnetic homogeneity of the samples. After integration and subtraction of the background, the experimental spectra were fitted to multipeak Lorentzian functions to obtain the resonance fields for each mode.

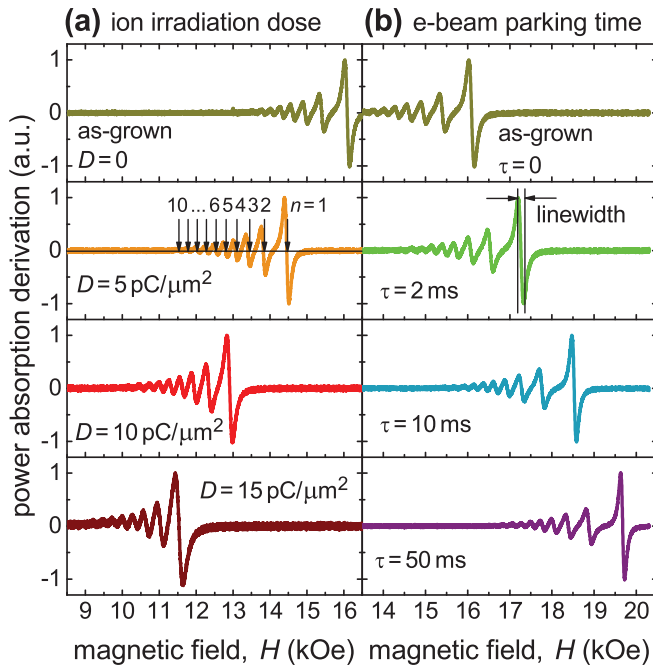


FIG. 2. Experimentally measured SWR spectra at 9.85 GHz for a series of 40-nm-thick Co-Fe disks with radius $R = 500$ nm irradiated with Ga ions at different doses, as indicated (a) and deposited with different electron beam parking times (b). The resonance mode number n and the peak-to-peak resonance linewidth are indicated.

A theoretical model⁵¹ was applied to fit the experimental data using M_s and A as two fitting parameters and assuming the gyromagnetic ratio of $\gamma/2\pi = 3.05$ MHz/Oe.⁵² In the [supplementary material](#), we demonstrate that a variation of the gyromagnetic ratio by 3% in the fits is equivalent to a variation of M_s and A by less than 1% so that the gyromagnetic ratio is assumed to be constant for all samples. In consequence of the ion-irradiation etching of the disks from the second series, we used 39, 38, and 37 nm for their thicknesses after the irradiation steps D_1 – D_3 , respectively. The application of a least-squares algorithm allowed us to deduce the magnetic parameters for all individual nanodisks with a precision of about 5%. [Figure 3](#) illustrates that the best theoretical fits (solid lines) nicely describe the experimental data (symbols). We note that the location of the main resonance peak is primarily determined by M_s . The value of A only weakly affects the position of the main resonance peak; however, it strongly affects the positions of the higher-order peaks.

The deduced M_s and A values are reported in [Figs. 4\(a\)](#) and [4\(b\)](#). The field-sweep resonance linewidth, determined as the peak-to-peak distance in [Fig. 2\(b\)](#), is presented in [Fig. 4\(c\)](#). We next analyze their evolution in comparison with the composition of the disks inferred from energy-dispersive x-ray (EDX) spectroscopy. The EDX was done at 3 kV/1.6 nA, corresponding to a disk thickness emitting x rays of about 35 nm, as estimated by Monte Carlo simulations (Casino). While the probed layer thickness should be smaller than the disk thickness in all cases, the open symbols in [Fig. 4\(d\)](#) represent the corrected data where the potential oxygen loss from the substrate (+3 at. % after each irradiation step) is taken into

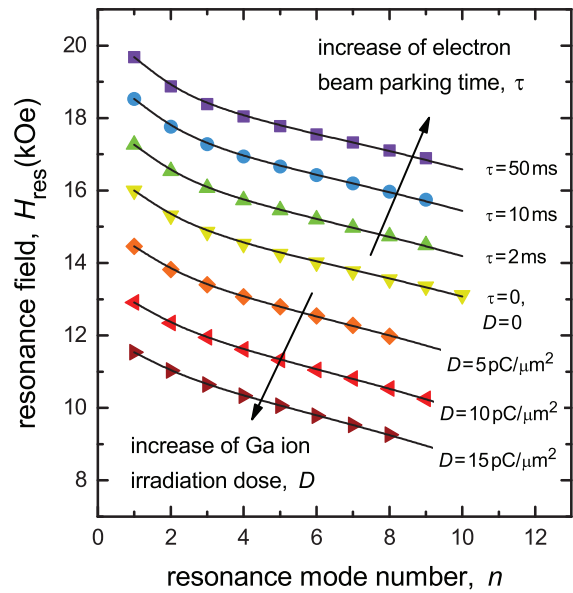


FIG. 3. Dependences of the resonance field H_{res} on the spin-wave mode number n for the disks irradiated with Ga ions at different doses and disks deposited with different parking times of the electron beam after each pass. Symbols: experiment. Solid lines: fits to the analytical theory⁵¹ with the magnetization M_s and the exchange constant A varied as fitting parameters, as reported in [Fig. 4](#), and the gyromagnetic ratio $\gamma/2\pi = 3.05$ MHz/Oe.

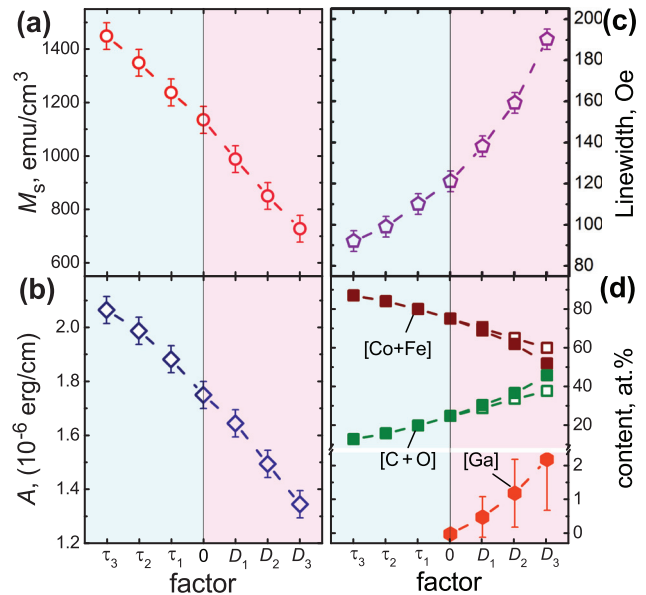


FIG. 4. Evolution of the magnetization M_s (a), the exchange constant A (b), the linewidth (c), and the disk composition (d) with the increase in the electron beam waiting time (τ_1 – τ_3 , light blue background) and the Ga ion irradiation dose (D_1 – D_3 , light magenta background). In (d), open symbols are the data correction accounting for a possible oxygen loss from the substrate by +3 at. % after each irradiation step. Dashed lines are guides to the eye.

account. The EDX data in Fig. 4(d) reveal an increase in the [Co+Fe] content from about 75 at. % in the reference sample ($\tau_0 = 0$) to about 87 at. % for the sample written with the beam parking time $\tau_3 = 50$ ms, Fig. 4(d). The increase in the metal content correlates well with the increase in M_s and A and the decrease in the linewidth in Fig. 4. In contrast, irradiation with Ga ions causes a degradation of the magnetic properties of the nanodisks, leading to a reduction of M_s and A , and an increase in the linewidth.

The particular values of τ and D were chosen as a scale factor in Fig. 4 to demonstrate in one plot the opposite character of the used approaches and the whole tuning range of M_s and A for Co-Fe nanostructures. The data in Fig. 4(a) suggest that M_s can be varied by a factor of about two, which offers sufficient flexibility, e.g., for the design of graded-index magnonic conduits^{23,26,27} and magnonic crystals.^{11,13,14} The data in Figs. 4(c) and 4(d) indicate that a decrease in the metal content in the disks by about 35 at. % is accompanied by a factor-of-two linewidth broadening. Yet, we note that the linewidth (90 Oe at 9.85 GHz) in the most CoFe-rich disk is a factor of about two larger than in sputtered Py films.⁵³

Regarding the physical reason for the larger M_s and A in the disks written with longer e-beam waiting time, we need to set into perspective the frequent observation that the metal content tends to increase with increasing beam current in the depleted regime,⁵⁴ and our observation that the metal content—and thus M_s and A —increases with increasing beam waiting time. From our recent study on the average precursor residence time of $\text{HCO}_3\text{Fe}(\text{CO})_{12}$,⁵⁵ we can calculate that the stationary precursor coverage under the growth conditions used here is only about 0.0065 monolayers, which is depleted in a beam dwell event by about 40%. With a calculated average residence time at room temperature of about 17 μs and a loop time of 490 μs , precursor replenishment is already completed within one loop. We thus conclude that the effect of the additional waiting time for the disks studies here is not that of precursor replenishment. We rather speculate that the waiting time allows for a more complete thermally induced carbonyl ligand desorption, resulting in an increased metal content.

As for the smaller M_s and A in the irradiated disks, degradation of ferromagnetic properties in consequence of ion irradiation is a well-known effect.^{29–35} We note that ion irradiation can lead to a different microstructure from the original material, such as, e.g., changes in the lattice parameter, grain sizes, and new phase formation.³¹ While an irradiation-induced increase in the surface roughness has been revealed by AFM, a comprehensive microstructural characterization of ion-irradiated Co-Fe has to remain for further investigations.

To summarize, we have demonstrated a methodology for the magnetization and exchange stiffness engineering in Co-Fe nanodisks. The disks were fabricated by the direct-write nanofabrication technology of focused electron beam-induced deposition. The analysis of the perpendicular SWR measurement data revealed an increase in the magnetization M_s and the exchange stiffness A in the disks written with longer e-beam waiting time and a reduction of M_s and A in disks irradiated with Ga ions. The decrease in M_s and A in conjunction with the linewidth increase reflects a degradation of the magnetic properties and a higher inhomogeneity of the disks irradiated with Ga ions. Specifically, the achieved variation of M_s from about 720 emu/cm^3 to about 1430 emu/cm^3 allows for its engineering in a broad range, continuously bridging the gap between the M_s values of widely used magnonic materials such as Py and CoFeB.¹⁵ In conjunction with a

spin-wave decay length in the range of 5–7 μm ,²⁴ this makes Co-Fe an interesting material for nanomagnonics. The M_s tuning is accompanied by a variation of the exchange stiffness in the range of 1.35×10^{-6} erg/cm to 2.07×10^{-6} erg/cm and the field-sweep FMR linewidth between 190 Oe and 90 Oe. The reported approach opens a way toward nanoscale 2D and 3D systems with fully controllable and space-varying magnetic properties.

See the [supplementary material](#) for Fig. S1, which illustrates the accuracy of the determination of M_s and A upon variation of the gyromagnetic ratio and the disk thickness.

The authors are very grateful to Sven Barth (Goethe University Frankfurt) for providing the precursor. O.V.D. acknowledges the Austrian Science Fund (FWF) for support through Grant No. I 4889 (CurviMag). The Portuguese team acknowledges the Network of Extreme Conditions Laboratories-NECL and Portuguese Foundation of Science and Technology (FCT) support through Project Nos. NORTE-01-0145-FEDER-022096, POCI-0145-FEDER-030085 (NOVAMAG), PTDC/FIS-MAC/31302/2017, and EXPL/IF/00541/2015. B.B. acknowledges financial support from the Vienna Doctoral School in Physics (VDSP). K.L. and A.V.C. acknowledge the Austrian Science Fund (FWF) for support through Grant No. I 4696. K.Y.G. acknowledges support from IKERBASQUE (the Basque Foundation for Science). The work of K.Y.G. was supported by the Spanish Ministerio de Ciencia, Innovación y Universidades Grant No. FIS2016-78591-C3-3-R. A.V.C. and Q.W. acknowledge support within the ERC Starting Grant No. 678309 MagnonCircuits. Support through the Frankfurt Center of Electron Microscopy (FCEM) is gratefully acknowledged. Furthermore, support from the European Cooperation in Science and Technology via COST Action No. CA16218 (NANOCOHBRI) is acknowledged.

DATA AVAILABILITY

The data that support the findings of this study are available within the article and its [supplementary material](#).

REFERENCES

- ¹V. V. Kruglyak, S. O. Demokritov, and D. Grundler, *J. Phys. D* **43**, 264001 (2010).
- ²*Magnonics*, edited by S. O. Demokritov and A. N. Slavin (Springer Berlin Heidelberg, 2013).
- ³A. V. Chumak, V. I. Vasyuchka, A. A. Serga, and B. Hillebrands, *Nat. Phys.* **11**, 453 (2015).
- ⁴K. Wagner, A. Kákay, K. Schultheiss, A. Henschke, T. Sebastian, and H. Schultheiss, *Nat. Nanotechnol.* **11**, 432 (2016).
- ⁵O. V. Dobrovolskiy, R. Sachser, T. Brächer, T. Böttcher, V. V. Kruglyak, R. V. Vovk, V. A. Shklovskij, M. Huth, B. Hillebrands, and A. V. Chumak, *Nat. Phys.* **15**, 477 (2019).
- ⁶*Spintronics Handbook: Spin Transport and Magnetism*, edited by E. Tsymbal and I. Zutic (CRC Press, Boca Raton, Florida, 2019).
- ⁷*Three-Dimensional Magnonics: Layered, Micro- and Nanostructures*, edited by G. Gubbiotti (Jenny Stanford Publishing, 2019).
- ⁸A. Mahmoud, F. Ciubotaru, F. Vanderveken, A. V. Chumak, S. Hamdioui, C. Adelman, and S. Cotozana, *J. Appl. Phys.* **128**, 161101 (2020).
- ⁹Q. Wang, M. Kewenig, M. Schneider, R. Verba, F. Kohl, B. Heinz, M. Geilen, M. Mohseni, B. Lägél, F. Ciubotaru, C. Adelman, C. Dubs, S. D. Cotozana, O. V. Dobrovolskiy, T. Brächer, P. Pirro, and A. V. Chumak, *Nat. Electron.* **3**, 765–774 (2020).

- ¹⁰Y. Li, W. Zhang, V. Tyberkevych, W.-K. Kwok, A. Hoffmann, and V. Novosad, *J. Appl. Phys.* **128**, 130902 (2020).
- ¹¹M. Krawczyk and D. Grundler, *J. Phys.: Condens. Matter* **26**, 123202 (2014).
- ¹²G. N. Kakazei, X. M. Liu, J. Ding, and A. O. Adeyeye, *Appl. Phys. Lett.* **104**, 042403 (2014).
- ¹³A. V. Chumak, A. A. Serga, and B. Hillebrands, *J. Phys. D: Appl. Phys.* **50**, 244001 (2017).
- ¹⁴H. Zakeri, *J. Phys.: Condens. Matter* **32**, 363001 (2020).
- ¹⁵M. Krawczyk and H. Puzskarski, *Phys. Rev. B* **77**, 054437 (2008).
- ¹⁶M. Yan, C. Andreas, A. Kakay, F. Garcia-Sanchez, and R. Hertel, *Appl. Phys. Lett.* **99**, 122505 (2011).
- ¹⁷A. V. Chumak, T. Neumann, A. A. Serga, B. Hillebrands, and M. P. Kostylev, *J. Phys. D: Appl. Phys.* **42**, 205005 (2009).
- ¹⁸X. M. Liu, J. Ding, G. N. Kakazei, and A. O. Adeyeye, *Appl. Phys. Lett.* **103**, 062401 (2013).
- ¹⁹I. A. Golovchanskiy, N. N. Abramov, V. S. Stolyarov, V. V. Bolginov, V. V. Ryazanov, A. A. Golubov, and A. V. Ustinov, *Adv. Funct. Mater.* **28**, 1802375 (2018).
- ²⁰N. I. Polushkin, V. Oliveira, O. Conde, R. Vilar, Y. N. Drozdov, A. Apolinário, A. García-García, J. M. Teixeira, and G. N. Kakazei, *Appl. Phys. Lett.* **101**, 132408 (2012).
- ²¹O. Dzyapko, I. V. Borisenko, V. E. Demidov, W. Pernice, and S. O. Demokritov, *Appl. Phys. Lett.* **109**, 232407 (2016).
- ²²M. Vogel, R. Aßmann, P. Pirro, A. V. Chumak, B. Hillebrands, and G. von Freymann, *Sci. Rep.* **8**, 11099 (2018).
- ²³P. Gruszecki and M. Krawczyk, *Phys. Rev. B* **97**, 094424 (2018).
- ²⁴O. V. Dobrovolskiy, R. Sachser, S. A. Bunyaev, D. Navas, V. M. Bezv, M. Zelent, W. Smigaj, J. Rychly, M. Krawczyk, R. V. Vovk, M. Huth, and G. N. Kakazei, *ACS Appl. Mater. Interfaces* **11**, 17654 (2019).
- ²⁵K. Baumgaertl, S. Watanabe, and D. Grundler, *Appl. Phys. Lett.* **112**, 142405 (2018).
- ²⁶C. S. Davies, A. Francis, A. V. Sadovnikov, S. V. Chertopalov, M. T. Bryan, S. V. Grishin, D. A. Allwood, Y. P. Sharaevskii, S. A. Nikitov, and V. V. Kruglyak, *Phys. Rev. B* **92**, 020408 (2015).
- ²⁷N. J. Whitehead, S. A. R. Horsley, T. G. Philbin, and V. V. Kruglyak, *Phys. Rev. B* **100**, 094404 (2019).
- ²⁸R. Bali, S. Wintz, F. Meutzner, R. Hübner, R. Boucher, A. A. Ünal, S. Valencia, A. Neudert, K. Potzger, J. Bauch, F. Kronast, S. Facsko, J. Lindner, and J. Fassbender, *Nano Lett.* **14**, 435 (2014).
- ²⁹M. Urbanek, L. Flajsman, V. Krizakova, J. Gloss, M. Horky, M. Schmid, and P. Varga, *APL Mater.* **6**, 060701 (2018).
- ³⁰P. Hartemann, *J. Appl. Phys.* **62**, 2111 (1987).
- ³¹D. Ozkaya L, R. M. Langford, W. L. Chan, and A. K. Petford-Long, *J. Appl. Phys.* **91**, 9937 (2002).
- ³²M. Langer, A. Neudert, J. I. Mönch, R. Mattheis, K. Lenz, J. Fassbender, and J. McCord, *Phys. Rev. B* **89**, 064411 (2014).
- ³³W. T. Ruane, S. P. White, J. T. Brangham, K. Y. Meng, D. V. Pelekhov, F. Y. Yang, and P. C. Hammel, *AIP Adv.* **8**, 056007 (2018).
- ³⁴A. Wawro, Z. Kurant, M. Jakubowski, M. Tekielak, A. Pietruczik, R. Böttger, and A. Maziewski, *Phys. Rev. Appl.* **9**, 014029 (2018).
- ³⁵V. Ahrens, S. Mendisch, W. Kaiser, M. Kiechle, S. Breitreutz-V Gamm, and M. Becherer, *J. Magn. Magn. Mater.* **523**, 167591 (2021).
- ³⁶M. Huth, F. Porrati, and O. V. Dobrovolskiy, *Microelectr. Eng.* **185–186**, 9 (2018).
- ³⁷F. Porrati, M. Pohlit, J. Müller, S. Barth, F. Biegger, C. Gspan, H. Plank, and M. Huth, *Nanotechnology* **26**, 475701 (2015).
- ³⁸A. Lara, O. V. Dobrovolskiy, J. L. Prieto, M. Huth, and F. G. Aliev, *Appl. Phys. Lett.* **105**, 182402 (2014).
- ³⁹E. Begun, O. V. Dobrovolskiy, M. Kompaniits, C. Gspan, H. Plank, and M. Huth, *Nanotechnology* **26**, 075301 (2015).
- ⁴⁰O. V. Dobrovolskiy, M. Kompaniits, R. Sachser, F. Porrati, C. Gspan, H. Plank, and M. Huth, *Beilstein J. Nanotechnol.* **6**, 1082 (2015).
- ⁴¹A. Fernandez-Pacheco, L. Skoric, J. De Teresa, J. Pablo-Navarro, M. Huth, and O. V. Dobrovolskiy, *Materials* **13**, 3774 (2020).
- ⁴²F. Porrati, S. Barth, R. Sachser, O. V. Dobrovolskiy, A. Seybert, A. S. Frangakis, and M. Huth, *ACS Nano* **13**, 6287 (2019).
- ⁴³O. V. Dobrovolskiy, E. Begun, M. Huth, V. A. Shklovskij, and M. I. Tsidlekh, *Physica C* **471**, 449 (2011).
- ⁴⁴O. V. Dobrovolskiy, V. M. Bezv, M. Y. Mikhailov, O. I. Yuzepovich, V. A. Shklovskij, R. V. Vovk, M. I. Tsidlekh, R. Sachser, and M. Huth, *Nat. Commun.* **9**, 4927 (2018).
- ⁴⁵O. V. Dobrovolskiy, V. M. Bezv, E. Begun, R. Sachser, R. V. Vovk, and M. Huth, *Phys. Rev. Appl.* **11**, 054064 (2019).
- ⁴⁶A. Fernández-Pacheco, R. Streubel, O. Fruchart, R. Hertel, P. Fischer, and R. P. Cowburn, *Nat. Commun.* **8**, 15756 (2017).
- ⁴⁷R. Streubel, P. Fischer, F. Kronast, V. P. Kravchuk, D. D. Sheka, Y. Gaididei, O. G. Schmidt, and D. Makarov, *J. Phys. D* **49**, 363001 (2016).
- ⁴⁸D. D. Sheka, O. V. Pylypovskiy, P. Landeros, Y. Gaididei, A. Kákay, and D. Makarov, *Commun. Phys.* **3**, 128 (2020).
- ⁴⁹O. V. Dobrovolskiy, S. A. Bunyaev, N. R. Vovk, D. Navas, P. Gruszecki, M. Krawczyk, R. Sachser, M. Huth, A. V. Chumak, K. Y. Guslienko, and G. N. Kakazei, *Nanoscale* **12**, 21207 (2020).
- ⁵⁰T. P. Ragesh Kumar, I. Unlu, S. Barth, O. Ingólfsson, and D. H. Fairbrother, *J. Phys. Chem. C* **122**, 2648 (2018).
- ⁵¹G. N. Kakazei, P. E. Wigen, K. Y. Guslienko, V. Novosad, A. N. Slavin, V. O. Golub, N. A. Lesnik, and Y. Otani, *Appl. Phys. Lett.* **85**, 443 (2004).
- ⁵²M. Tokac, S. A. Bunyaev, G. N. Kakazei, D. S. Schmool, D. Atkinson, and A. T. Hindmarch, *Phys. Rev. Lett.* **115**, 056601 (2015).
- ⁵³S. S. Kalarickal, P. Krivosik, M. Wu, C. E. Patton, M. L. Schneider, P. Kabos, T. J. Silva, and J. P. Nibarger, *J. Appl. Phys.* **99**, 093909 (2006).
- ⁵⁴W. F. van Dorp and C. W. Hagen, *J. Appl. Phys.* **104**, 081301 (2008).
- ⁵⁵M. Huth, F. Porrati, P. Gruszka, and S. Barth, *Micromachines* **11**, 28 (2019).